ACS Catalysis

Research Article

pubs.acs.org/acscatalysis

Preparation of Fischer–Tropsch Supported Cobalt Catalysts Using a New Gas Anti-Solvent Process

Raimon P. Marin,[†,§] Simon A. Kondrat,[†] James R. Gallagher,[‡] Dan I. Enache,[§] Paul Smith,[†] Paul Boldrin,[‡] Thomas E. Davies,[†] Jonathan K. Bartley,[†] Garry B. Combes,[§] Peter B. Williams,[§,∥] Stuart H. Taylor,[†] John B. Claridge,[‡] Matthew J. Rosseinsky,[‡] and Graham J. Hutchings*[,†]

[†]Cardiff Catalysis Institute, School of Chemistry, Cardiff University, Main Building, Park Place, Cardiff, CF10 3AT, U.K.

[‡]Department of Chemistry, University of Liverpool, Crown Street, Liverpool L69 7ZD, U.K.

[§]Johnson Matthey Plc., P.O. Box 1, Belasis Avenue, Billingham, Cleveland, TS23 1LB, U.K.

Supporting Information

ABSTRACT: Cobalt and ruthenium-promoted cobalt Fischer–Tropsch catalysts supported on titania have been prepared for the first time by gas anti-solvent precipitation. The use of dense CO_2 as an anti-solvent enables the precipitation of cobalt acetate and ruthenium acetylacetonate onto preformed titania. The gas anti-solvent process produces catalysts with the desired 20 wt % cobalt content as precursors, which on calcination give highly dispersed Co_3O_4. The addition of ruthenium to the gas anti-solvent prepared cobalt catalysts has been investigated by two methods (a) coprecipitation with cobalt acetate and (b) wet impregnation onto a precalcined cobalt titania catalyst, and these resulted in catalysts with distinctly different properties. These catalysts were compared with a standard ruthenium-promoted cobalt catalyst prepared by wet impregnation and were found to be substantially more active for the Fischer–Tropsch reaction.

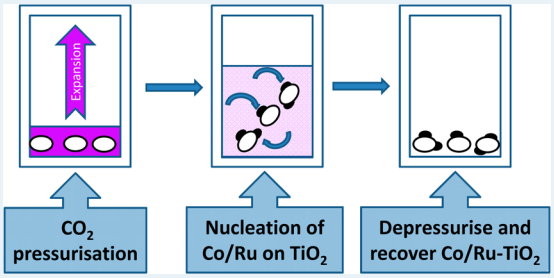

KEYWORDS: *Fischer–Tropsch, cobalt, ruthenium, cobalt acetate, supercritical anti-solvent precipitation*

INTRODUCTION

Fischer–Tropsch (FT) chemistry is undergoing a resurgence because of diminishing oil reserves and the potential to utilize alternative fuel sources, such as biomass. Supported cobalt nanoparticles are frequently used as an FT catalyst because of their resistance to deactivation and efficiency for long chain hydrocarbon synthesis.[1,2] Activity has been noted to be influenced by a number of factors, including cobalt particle size, dispersion, reducibility, and the support used.[3−6] However, the situation is further complicated as the reaction conditions can influence the structure sensitivity of the reaction. Iglesia et al. demonstrated that, at high conversions under high pressure conditions chosen to favor chain growth (>5 bar), turnover rates are not influenced by cobalt dispersion or support effects.[7,8] Promoter materials, such as Ru, Re, Pt, and Pd are also well-known to affect the catalyst properties and consequently the activity and selectivity.[6,9,10] In addition to these parameters, different catalyst preparation methods and precursors influence cobalt particle properties and their interaction with supports and promoters.

Aqueous impregnation of a support with cobalt nitrate and promoter salts, either by co-impregnation or sequential addition, followed by calcination, is the most common preparation method.[1] Adaptations of impregnation preparations include the use of different cobalt salts,[1,11] specifically cobalt acetate[12] and the use of chelating agents to influence dispersion.[13] Other catalyst preparation methods investigated include deposition precipitation of cobalt onto supports and sol–gel preparation methods.[14,15]

The use of gas anti-solvent (GAS) and supercritical anti-solvent (SAS) precipitation as a method of catalyst synthesis offers a route to novel materials, with properties intrinsic to the method of preparation. Both techniques use dense gases near or above their critical point as an anti-solvent to precipitate a substrate, which is insoluble in the supercritical fluid, from a solution where the solvent is miscible. Carbon dioxide has most commonly been used because it is inexpensive, relatively nontoxic, and easy to reuse.[16,17] GAS precipitation involves the gradual addition of CO_2 to a closed batch system containing the solution, as the pressure increases the miscibility of CO_2 with the solvent also increases causing a volumetric expansion, resulting in supersaturation and nucleation of the solute.[18] SAS precipitation involves the constant addition of the solvent, via a nozzle, to the supercritical CO_2 in a semicontinuous process. The mixing of the two phases results in rapid diffusion and precipitation of the solute.[18] These anti-solvent processes are not to be confused with methods that use supercritical media as the solvent, such as the rapid expansion supercritical solution

Received: January 18, 2013
Revised: February 21, 2013
Published: March 6, 2013

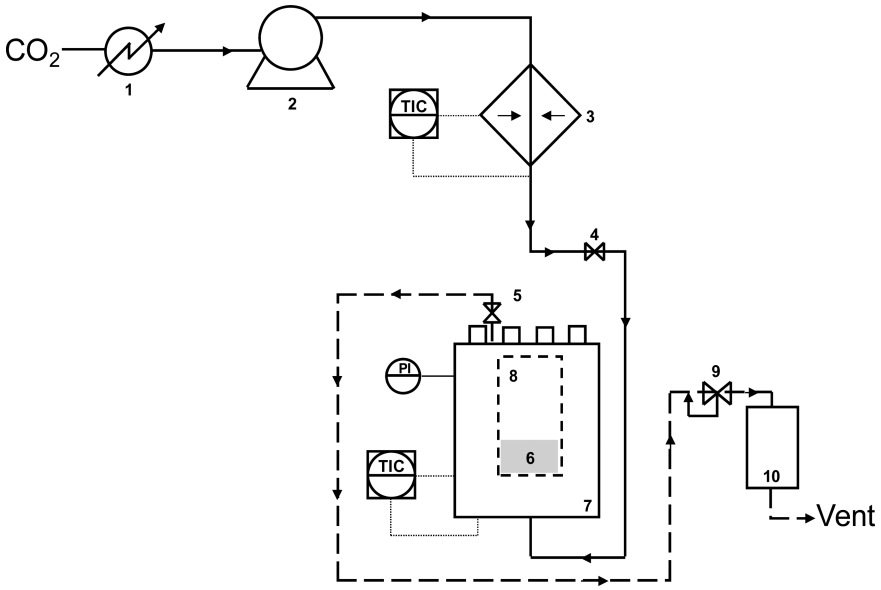

Figure 1. Schematic of the Separex apparatus for preparation of GAS materials. Key: (1) CO_2 chiller system; (2) CO_2 pump; (3) CO_2 heat exchanger; (4) Isolation valve; (5) Valve to change to the flow system for washing step; (6) Preloaded metal salt solution; (7) Heating jacket; (8) Precipitation chamber; (9) Back pressure regulator; (10) Solvent recovery pot: (TIC) temperature controller; (PI) pressure indicator.

(RESS) and supercritical deposition techniques.[19,20] Although these techniques have successfully produced supported and unsupported nanoparticles, they suffer from the limited solubility of affordable salts in desirable supercritical fluids, for example, CO_2 or water.

SAS and GAS processes have been successfully used in the preparation of nanoparticular pharmaceuticals, polymers, metal pigments, and semiconductor materials.[21−24] Catalyst preparation by SAS precipitation has been demonstrated for various materials over the past decade. Single metal oxide supports prepared by SAS, such as TiO_2 and CeO_2, have been shown to facilitate high dispersion of active metals, consequently producing high turnover rates for several catalytic reactions.[25,26] In addition, the SAS process has been used to prepare mixed metal oxide catalysts, such as $CuMnO_x$ which has been shown to be highly active for CO oxidation.[27−30]

To date, catalyst preparation using the CO_2 anti-solvent process has involved the simultaneous precipitation of metal salts by SAS, which is analogous to standard coprecipitation techniques. The current work discussed in this communication applies the CO_2 anti-solvent precipitation of metal salts to a system that also contains a preformed support material, in the batch GAS process. This process is most comparable with a wet impregnation technique, used frequently for FT catalyst preparation. Supercritical deposition of metal salts onto support materials clearly has some equivalence to GAS precipitation with a preformed support material. However, as mentioned previously, the difference is that in the GAS technique the supercritical or dense gas is used as an anti-solvent and not a solvent as it is with deposition techniques. The advantage of GAS is that it does not require expensive and complex metal salts. The result of this new GAS preparation process is the formation of cobalt and cobalt/FT promoter mixtures supported on TiO_2. The prepared materials have been fully characterized and tested for FT synthesis.

EXPERIMENTAL SECTION

Catalyst Preparation. Catalysts were prepared by gas anti-solvent precipitation using equipment provided by Separex S.A. (see Figure 1). Cobalt(II) acetate tetrahydrate (Sigma Aldrich ACS, ≥98% purity) solution in methanol (Fischer, reagent grade) (100 mL, 54 mg mL^{-1}) was added to the precipitation vessel together with TiO_2 (50 mg mL^{-1}) (P25, Degussa). The target Co loading was 20 wt %. The vessel was then sealed and pressurized at a controlled rate of about 5 bar min^{-1} with the CO_2 inlet at the bottom to facilitate good mixing between the CO_2 and the solution. To further aid mixing overhead stirring was applied to the solution during the addition of CO_2. Prior to being introduced into the vessel the liquid CO_2 is chilled to −4 °C, so that it can be pressurized using a pump, before going through a heat exchanger to the desired 25 °C temperature. The system was pressurized to 80 bar, which was calculated to be a 900 vol % expansion of the precursor solution. The expansion of the solution, because of CO_2 incorporation, resulted in its supersaturation, with cobalt(II) acetate then nucleating at sites on the TiO_2 surface. Once the maximum pressure was attained the system was allowed to equilibrate for 10 min. Then CO_2, at the same pressure (80 bar) and temperature (25 °C), was passed through the system in a continuous flow of 12 L min^{-1} to remove the methanol. After depressurization the dry material was removed from the system and transferred to a Carbolite tube furnace for calcination in static air at 350 °C for 5 h. This material is denoted GAS Co/TiO_2.

The addition of 0.05 wt % Ru to the GAS Co-TiO_2 catalyst was performed using two different methods. Ru was introduced after calcination of the GAS Co/TiO_2 catalyst by wet impregnation using ruthenium(III) nitrosyl nitrate (Sigma Aldrich, 1.5 wt % Ru in nitric acid). This material was then calcined for a second time at 350 °C for 5 h and henceforth is called GAS Co/TiO_2 Ru IMP. A GAS coprecipitation of the cobalt(II) acetate tetrahydrate and ruthenium(III) acetylacetonate (Sigma Aldrich, purum ≥97%) was also performed, in which both salts nucleate onto the TiO_2 support from the

dx.doi.org/10.1021/cs4000359 | ACS Catal. 2013, 3, 764−772

supersaturated methanol-CO_2 solution. This material was then recovered and calcined at 350 °C for 5 h. Ruthenium(III) acetylacetonate is partially soluble in supercritical CO_2.[31] This low solubility meant that a higher amount of the Ru salt (1.2 mg mL^{-1}) was used in the methanol/CO_2 system to achieve a 0.5 wt % Ru loading in the final catalyst. This material was denoted GAS Co−Ru/TiO_2.

For comparison, a standard 20 wt % Co/0.05 wt % Ru on TiO_2 catalyst was prepared by wet coimpregnation using cobalt(II) nitrate hexahydrate (Alfa Aesar, >98%) and ruthenium(III) nitrosyl nitrate (>31.3% Ru, Alfa Aesar) with the TiO_2 support. The TiO_2 used was a commercial support designed for use in FT systems. The material was then calcined in static air at 250 °C for 8 h. The material is denoted as IMP Co−Ru/TiO_2.

Catalyst Characterization. Diffuse reflectance infrared spectroscopy (DRIFTS) was performed using a Bruker Tensor 27 with a HgCdTe (MCT) detector and a Harrick Praying Mantis HVC-DRP-4 cell with a ZnSe window. Inductively coupled plasma (ICP) analysis was performed using a Perkin-Elmer Optima 3300RL ICP-OES. X-ray diffraction (XRD) data were collected on a Panalytical X-Pert diffractometer with an X-Celerator detector and Co $K_{\alpha 1}$ radiation, using variable divergence slits with an illuminated length of 10 mm. Data was collected over a 2θ range 20−130°, with an effective step size of 0.017° and a counting time of 393 s/°. Materials Analysis Using Diffraction (MAUD), a Java based Rietveld refinement software, was used to fit the whole XRD pattern for each sample using an iterative least-squares method.[32,33] The instrumental contribution to the observed peak shape was determined using a line shape standard (LaB_6, NIST SRM 660a). In addition to background polynomial and offset, the following parameters were refined for each phase of each sample: weight fraction, lattice parameters, isotropic *Delf* particle size, thermal parameters, and fractional atomic coordinates.

Hydrogen chemisorption was performed using a Micromeritics ASAP 2020 apparatus, and used to elucidate the cobalt surface area of the prepared catalysts. To perform the analysis 0.5 g of the sample was reduced under pure H_2 at 425 °C for 6 h. Residual H_2 was removed from the system using vacuum >1 × 10^{-2} mbar at 450 °C for 2h. The temperature was then reduced to 150 °C and H_2 dosed over the sample in the pressure range of 130−1015 mbar.

The catalyst reducibility was investigated using temperature programmed reduction, which was performed using a Quatachrome ChemBET 3000. Samples of 50−150 mg were tested under an atmosphere of 10% H_2 in Ar (20 mL min^{-1}) from 50 °C up to 600 °C at a ramp rate of 5 °C min^{-1}.

Catalyst Testing. Catalysts were tested for the FT reaction in a fixed bed reactor consisting of 1/4″ I.D. stainless steel tubes housed within a forced N_2 recirculating furnace. Catalyst (0.13 g diluted with 0.5 g of SiC) was packed within the reactor and tested at temperatures in the range 210−245 °C at 20 bar pressure. The syngas mixture used was Ar:CO:H_2 = 1:1:2. Liquid and wax traps were situated post reactor to collect both the liquid and the wax products. Gaseous products were measured online by gas chromatography.

Testing was started at a GHSV of 28 L g_{cat}^{-1} h^{-1}, and after 24 h the syngas flow rate was adjusted so that all reactions were at 50% CO conversion. The selectivity was therefore compared under iso-conversion conditions. The flow rates required to achieve iso-conversion are given in the relevant figures that describe catalyst activities.

RESULTS AND DISCUSSION

Diffuse reflectance FT-IR of the GAS prepared samples, prior to calcination, is shown in Figure 2. This was performed to elucidate the effect of the GAS preparation on the metal salts used. The GAS prepared Co-TiO_2 and Co/Ru-TiO_2 materials had symmetric and asymmetric carbonyl bands at 1567 cm^{-1} and 1425 cm^{-1}, characteristic of the cobalt(II) acetate salt, as observed in the IR spectrum of the cobalt(II) acetate tetrahydrate starting material (Figure 2a). No evidence of the ruthenium(III) acetylacetonate was observed in the GAS Co−Ru/TiO_2 sample, as the loading was below the detection limit of the equipment. Interestingly, the positions of the acetate carbonyl bands varied subtly between the GAS prepared materials and the starting cobalt(II) acetate tetrahydrate, with the latter having bands at slightly lower wavenumbers. In addition to this, the distance between the symmetric and the asymmetric bands increased from 126 cm^{-1} in the starting cobalt(II) acetate tetrahydrate to 142 cm^{-1} for the GAS Co/TiO_2 and Co−Ru/TiO_2 materials. These variations are indicative of a subtle change in the binding co-ordination of the acetate anion to the cobalt ion.[34] When cobalt acetate was precipitated by GAS in the absence of the TiO_2 support it was found to give identical band positions to the GAS Co/TiO_2 and Co/Ru-TiO_2 materials, demonstrating that the change in co-ordination observed was due to the GAS precipitation and not from an interaction with the TiO_2 support.

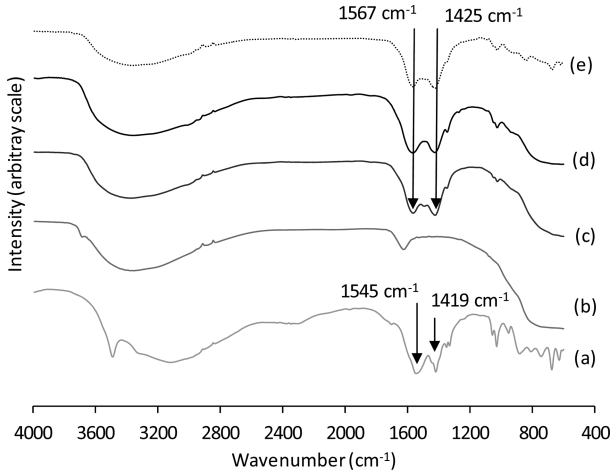

Figure 2. DRIFTS of the GAS catalyst precursors. (a) Standard cobalt(II) acetate tetrahydrate; (b) TiO_2 support; (c) GAS Co/TiO_2; (d), GAS Co−Ru/TiO_2; (e) GAS precipitated cobalt acetate.

ICP elemental analysis to determine Co and Ru content of the calcined GAS prepared and standard impregnation catalyst is shown in Table 1. All samples were found to have Co loadings within 2.5 wt % of the target loading of 20 wt %. GAS precipitation of Co onto the TiO_2 support, without the coprecipitation of the Ru salt, was very close to the theoretical loading. The addition of ruthenium(III) acetylacetonate in the coprecipitated GAS experiment resulted in a slight drop in the Co loading. As ruthenium(III) acetylacetonate is partially soluble in carbon dioxide it can alter the phase system in the GAS experiment, which could increase the solubility of cobalt acetate in the carbon dioxide anti-solvent.[31] The enhancement

dx.doi.org/10.1021/cs4000359 | ACS Catal. 2013, 3, 764−772

Table 1. ICP Elemental Analysis of Co and Ru Content in the Catalysts

sample	Co content (wt %) (±0.1 wt %[a])	Ru content (wt %) (±0.02 wt %[a])
IMP Co−Ru/TiO_2	17.5	0.03
GAS Co/TiO_2	20.6	0.00
GAS Co/TiO_2 Ru IMP	20.6	0.08
GAS Co−Ru/TiO_2	18.6	0.21

[a]Error calculated from repeat analysis.

in the solubility of one salt by another is well-known for supercritical systems and is known as the entrainer effect.[35] The successful loading of about 20 wt % Co onto the TiO_2 support demonstrates the capability of the GAS process to provide materials with high metal loadings. This level of loading is much more difficult to achieve with supercritical deposition techniques, because of salt solubility issues, with the highest reported Co loading by supercritical deposition being 5.1 wt % onto Al-MCM-41.[36]

Ru metal loadings of the catalysts were found to be more variable, with some loadings significantly deviating from the target 0.05 wt %. Where Ru was added by wet impregnation the variances observed were small and can be attributed to errors in the preparation technique, because of the very low loadings used, and in the elemental analysis. The loading was substantially higher in the GAS Co/Ru-TiO_2 sample, at 0.21 wt % which is due to an inaccurate estimation of the yield of Ru precipitation. The solubility of ruthenium(III) acetylacetonate in the complex CO_2-methanol-cobalt acetate phase was predicted to be high and so it was anticipated that the yield would be fairly low, whereas experimentally ∼40% of the Ru salt was found to precipitate. It is important to note that the successful coaddition of Co and Ru using a dense or supercritical CO_2 has not been previously reported, with supercritical deposition work focusing solely on Co deposition.[36] Ru has been reported as an active FT catalyst, with reported turnover rates comparable to those seen for Co.[8,10] Therefore, the excess Ru within the GAS Co/Ru-TiO_2 sample would not have a disproportionate effect on activity, when considered simply as an independent metal active phase. However, synergy is often observed with bimetallic Co and Ru catalysts, but with only small amounts of Ru at 0.05 to 0.1% being required.[9] A precise Co:Ru ratio for optimal activity is difficult to find in the literature as most studies use nonselective methods of adding Ru to catalysts with varying Co loadings and support structures. This results in considerable variation in Co−Ru interactions between studies. In addition promoter effects are strongly dependent on FT reaction pressure.[9]

Refinement of the XRD patterns (patterns shown in SOM Figures 1−4) for the calcined materials has been performed to provide weight fractions of phases, crystallite sizes, and lattice parameters. In all samples anatase and rutile TiO_2 phases were observed, along with the expected Co_3O_4 phase. An additional phase was observed in the GAS precipitated materials, which was assigned as a cobalt titanate phase that most closely matched Co_2TiO_4. However, the lattice parameters for the cobalt titanate phase, as measured by XRD, were smaller than that observed for Co_2TiO_4 in the literature (ICDD 00-039-1410), which indicates that the Co_2TiO_4 phase was in a solid solution with Co_3O_4. Parameters for Co_3O_4 and cobalt titanate phases are given in Table 2. In addition the weight fractions of Co_3O_4 were used to calculate the wt % Co contents, excluding Co from the titanate phase.

The calculated Co content from XRD analysis (Table 2) was found to be in broad agreement with the values from ICP (Table 1). However, the XRD derived loadings were found to be lower than ICP values by about 1 to 3.5 wt %. Co that was associated with a titanate phase has not been included in the XRD values, because of the unknown stoichiometry of the phase, which would in part account for lower calculated loadings. In addition, XRD analysis requires materials with long-range order, whereas isolated surface species and very small particles are difficult to detect. Therefore, Rietveld refinement tends to underestimate quantification of phases containing such particles. These analytical limitations contribute to lower than expected calculated Co loadings and made precise calculation of Co content in nonreducible titanate phases unfeasible.

The average Co_3O_4 crystallite size for the GAS prepared samples ranged between 16 and 20 nm, whereas the standard IMP Co−Ru/TiO_2 catalyst was calculated to have an average Co_3O_4 crystallite size of 36 nm. Girardon et al. showed that a cobalt acetate-SiO_2 impregnated precursor on calcination resulted in small amounts of poorly crystalline Co_3O_4, with significant amounts of Co_2SiO_4.[12] As large amounts of Co were incorporated into the SiO_2 it would be expected that remaining Co species would be poorly crystalline. The smaller Co_3O_4 crystallite sizes in the GAS materials could be attributed to the use of the cobalt acetate precursor. However, the relative composition of nonreducible Co_2SiO_4 to Co_3O_4 was high in the work of Girardon et al. whereas it was much lower in the GAS prepared Co/TiO_2 materials. Within the set of samples prepared by GAS, the Ru free catalyst had the smallest average Co_3O_4 crystallite size. Addition of Ru by impregnation required an additional calcination step, which can lead to sintering and the observed increase in the Co_3O_4 crystallite size. The largest crystallite size in the samples produced by GAS was for the coprecipitated ruthenium acetylacetonate and cobalt(II) acetate tetrahydrate. The disrupted phase system that resulted in a reduced Co yield, as observed by ICP, can also explain the

Table 2. Co_3O_4 and Co_2TiO_4 Phase Parameters and Estimated Co Loadings from Rietveld Refinement of XRD Analysis of the Catalysts[a]

sample	Co_3O_4 crystallite size (nm)	Co_3O_4 lattice parameter	Co_3O_4 weight fraction (wt %)	Cobalt titanate weight fraction (wt %)	calculated Co content from Co_3O_4 (wt %)
IMP Co−Ru/TiO_2	36.0 ± 0.2	8.080 ± 0.002	22.0 ± 0.2	0.00	16.1 ± 0.1
GAS Co/TiO_2	17.0 ± 0.2	8.099 ± 0.003	23.1 ± 0.3	8.4 ± 0.3	17.0 ± 0.2
GAS Co/TiO_2 Ru IMP	17.1 ± 0.1	8.100 ± 0.004	23.0 ± 0.3	4.9 ± 0.2	16.9 ± 0.2
GAS Co−Ru/TiO_2	20.2 ± 0.2	8.100 ± 0.003	23.3 ± 0.3	n/a	17.7 ± 0.2

[a]Quoted errors are estimates based on the standard uncertainty in the powder diffraction pattern intensities and should be considered as lower bounds.

dx.doi.org/10.1021/cs4000359 | ACS Catal. 2013, 3, 764−772

larger Co_3O_4 crystallite size. The enhanced solubility of cobalt acetate in the GAS system would result in a lower supersaturation of the solution, giving lower nucleation rates and facilitating crystal growth. This resulted in a poorer dispersion of cobalt acetate that on calcination produced a larger average Co_3O_4 crystallite size. It is worth noting that all the GAS samples have smaller particle sizes than the IMP Co−Ru/TiO_2 material, which suggests that reduced Co dispersion of the GAS samples would be higher than IMP Co−Ru/TiO_2, as previous studies have shown good agreement between Co_3O_4 particle size and Co dispersions.[37]

XRD analyses of the Co_3O_4 phases showed a larger than expected lattice parameter for all the GAS prepared samples. The lattice parameter in all the GAS preparations was 0.2 Å larger than that seen in bulk Co_3O_4 and the IMP Co−Ru/TiO_2 material. As this unit cell expansion was observed for samples with and without Ru addition, the incorporation of this metal into Co_3O_4 cannot be responsible for the observed expansion. This does not discount the possibility that Ru was incorporated into the lattice, but does demonstrate that an alternative effect is responsible for this observation. Nanoparticles can have different lattice parameters than bulk materials, but previous observations for nanoparticular Co_3O_4 have shown a contraction in lattice parameter.[38] An interaction between the Co_3O_4 and titania phases in the samples prepared by GAS could provide an explanation for the expanded unit cells.

The observation of a cobalt titanate phase in all GAS samples provides confirmation of an interaction between the cobalt and titania phases. For the GAS Co−Ru/TiO_2 sample, although peaks indicative of a titanate phase were present, they were too weak to refine, and Raman spectroscopy was used as a complementary technique to confirm its presence (Figure 3).

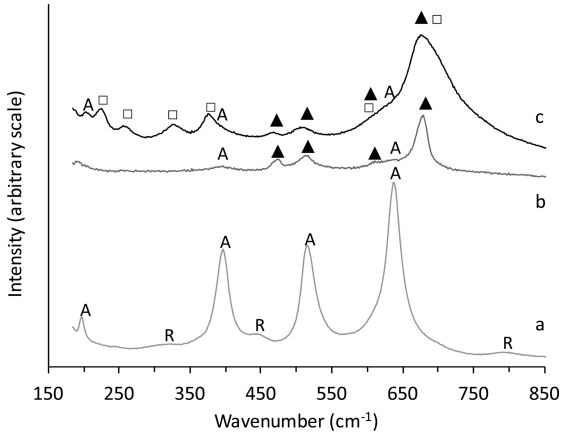

Figure 3. Raman spectra showing the presence of cobalt titanate in GAS Co−Ru/TiO_2. (a) TiO_2 support; (b) site 1 of GAS Co−Ru/TiO_2; (c) site 2 of GAS Co−Ru/TiO_2. Key: (R) rutile phase, (A) anatase phase, ▲ Co_3O_4, □ cobalt titanate.

The high dispersion of cobalt species on the surface of the titania, because of the higher nucleation rates in the GAS process, could be key to the cobalt titanate formation. During calcination the high surface interaction between titania and cobalt facilitates mass transfer of metal ions to form the mixed metal spinel. This ability to overcome the activation barrier to form a mixed metal oxide at relatively low temperatures, because of intimate mixing of metals, has been previously observed for CuMnOx systems prepared by SAS.[28] The exothermic decomposition of acetate salts could also play a role in facilitating metal ion migration.[12]

Although the presence of cobalt titanate is indicative of a high dispersion of Co species, the phase itself is detrimental to the Co metal surface area and consequently FT activity. Therefore, limiting cobalt titanate content is considered important in producing an active catalyst. The calculated weight fraction of cobalt titanate was lower in the GAS Co/TiO_2 Ru IMP to that seen in the GAS Co/TiO_2 sample. The inability to get a stable refinement of the cobalt titanate phase for the GAS Co−Ru/TiO_2 sample indicates an even smaller cobalt titanate weight composition, though care should be taken in this analysis as other factors, such as crystallite size, could be responsible. The ability of catalyst promoters, such as Ru, to inhibit formation of mixed cobalt support phases has been noted in the literature.[39] However, within this sample set it was observed that a decrease in cobalt titanate content corresponded with an increase in Co_3O_4 crystallite size. Therefore an alternative mechanism is proposed, that the lower cobalt titanate content is a result of a poorer dispersion of Co over the TiO_2 support.

Temperature programmed reduction (TPR) provides valuable information on the reducibility of the catalysts, the nature of the cobalt oxide phases present, and the interaction of these phases with the Ru promoter and the TiO_2 support. The temperature maxima (T_{max}) of the peaks seen in the reduction of the catalysts up to 600 °C are shown in Table 3 and Figure 4.

Table 3. Reduction Peaks from TPR Analysis of the Catalysts

sample	residual nitrate precursor T_{max} (°C)	Co_3O_4 → CoO T_{max} (°C)	CoO → Co T_{max} (°C)
IMP Co−Ru/TiO_2	209	293	406
IMP Co/TiO_2	206	310	415 and 465
GAS Co/TiO_2		330	444
Co/TiO_2 Ru IMP		186	303
GAS Co−Ru/TiO_2		244	354

All of the GAS prepared samples show two peaks associated with the reduction of Co_3O_4 to CoO and the reduction of CoO to Co respectively.[40] The standard impregnation catalyst with Ru showed an additional low temperature reduction peak (Figure 4a) which has been assigned to residual nitrates from

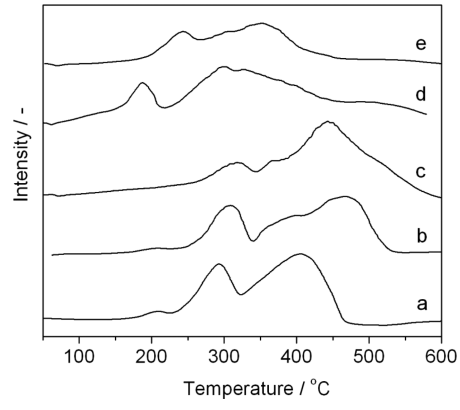

Figure 4. TPR analysis of the catalysts. (a) IMP Co−Ru/TiO_2; (b) IMP Co/TiO_2; (c) GAS Co/TiO_2; (d) GAS Co/TiO_2 Ru IMP; (e) GAS Co−Ru/TiO_2.

dx.doi.org/10.1021/cs4000359 | ACS Catal. 2013, 3, 764−772

catalyst preparation.[12] A comparable impregnation material without Ru had an additional high temperature CoO to Co reduction peak attributed to well dispersed cobalt oxide particles (Figure 4b). The reduction of cobalt titanate was not observed in the TPR experiments as the maximum temperature investigated was 600 °C, while cobalt titanates are known to require temperatures of around 700 °C to reduce. An additional TPR experiment was performed, seen in Figure 5,

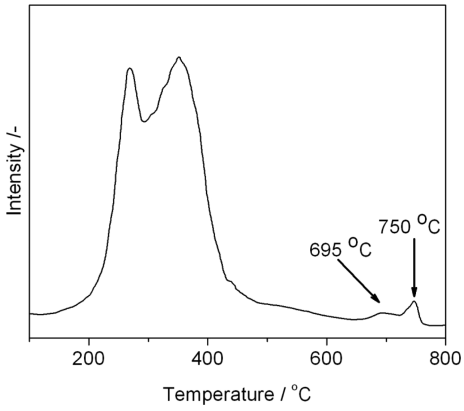

Figure 5. TPR analysis of GAS Co−Ru/TiO_2 over an extended temperature range (25−800 °C).

on the Co/Ru-TiO_2 GAS sample up to 800 °C to observe the cobalt titanate reduction. This showed a reduction peak at 700 °C, which further enforces the interpretation that cobalt titanate is present from the XRD and Raman data. TPR analysis to determine cobalt content in a titanate phase is of limited use, as high temperature analysis will affect the catalyst structure and also facilitate TiO_2 reduction.[1,41]

The addition of Ru to the samples resulted in a decrease in the reduction temperature of the Co oxide phases, which is in agreement with Co−Ru systems in the literature.[7,9,10] However, the extent of this temperature shift varied considerably between the samples. The Ru containing IMP Co−Ru/TiO_2 catalyst showed a highest reduction maxima about 60 °C lower than a comparable catalyst prepared without Ru. The simultaneous GAS precipitation of Co and Ru resulted in a temperature shift of about 90 °C from the unpromoted Co catalyst, while the addition of Ru by impregnation to the GAS Co/TiO_2 had a more significant temperature reduction of about 140 °C. Differences in Co_3O_4 crystallite size and weight fraction of the GAS materials, seen by XRD, were considered too minimal to be responsible for the dramatic difference in reduction temperature. In light of this, the variation is assigned to differences in the Co−Ru interaction that arise from the differing preparation conditions. The enhanced reducibility of cobalt oxide with noble metals can be explained by two different phenomena. Noble metal oxides are known to reduce at lower temperature than cobalt oxide and the subsequent noble metal would then facilitate hydrogen dissociation, which enhances cobalt oxide reduction by hydrogen spillover.[9] The other phenomenon is associated with the formation of bimetallic Ru−Co oxide particles which have a greater reduction potential.[9,10] The two different routes of Ru addition in the GAS catalysts would be expected to offer differing degrees of Co and Ru mixing. The sequential addition of Ru by impregnation in the GAS Co/TiO_2 Ru IMP catalyst would result in phase separated Ru and Co_3O_4, although the subsequent heat treatment could result in a partial migration of Ru into the Co_3O_4. The simultaneous precipitation of Co and Ru salts in the GAS Co−Ru/TiO_2 would be likely to result in homogeneously mixed Co and Ru, as supercritical anti-solvent processes are known to give exceptionally good mixing.[29] This suggests that Ru−Co mixed oxides are likely to form in the GAS precipitated material, whereas surface Ru is more likely to form in the impregnated material. This implies that a hydrogen spill over mechanism is more dominant in the GAS Co/TiO_2 Ru IMP catalyst, and this provides a greater enhancement in cobalt oxide reduction.

Dispersion of Co on the catalysts, which had been reduced at 425 °C, is shown in Table 4. It was noted that the unpromoted

Table 4. Cobalt Dispersions of the Catalysts

sample	Co dispersion (%)
IMP Co−Ru/TiO_2	1.8
GAS Co/TiO_2	1.3
GAS Co/TiO_2 Ru IMP	2.9
GAS Co−Ru/TiO_2	3.9

GAS Co/TiO_2 had a significantly lower Co surface area compared with the other GAS prepared catalysts. Co surface area is proportional to degree of reduction and Co loading, and inversely proportional to Co particle size; given the similarity of the cobalt loading and particle size, it is clear that the lower surface area is due to its poorer reduction behavior, as shown by TPR. A comparison of the Ru promoted GAS catalysts and the Ru promoted standard impregnation catalyst shows significantly higher cobalt surface areas for catalysts prepared by GAS (Figure 6). An 11 wt % Co, Ru promoted, wet impregnation catalyst produced by Iglesia et al. had a dispersion of 2.6%[10] compared to the IMP Co−Ru/TiO_2 materials' 1.8% dispersion. Taking into account that the 40% higher loading in the IMP Co−Ru/TiO_2 material would hinder dispersion, its Co dispersion can be considered reasonable for an impregnation technique. The higher dispersions of GAS catalysts agrees with the assumption made from the calculated Co_3O_4 crystallite sizes, that preparation by GAS precipitation afforded a better dispersion of Co precursor species. In addition TPR showed that, while the standard impregnation catalyst was more reducible than the unpromoted (nonpromoted) GAS Co/TiO_2 catalyst, it was significantly less reducible than the Ru promoted GAS catalysts.

The higher Co dispersion of GAS Co−Ru/TiO_2, compared with the GAS Co/TiO_2 Ru IMP catalyst, cannot be explained by the degree of cobalt oxide reduction that has occurred. As the GAS Co/TiO_2 Ru IMP was found to have smaller CO_3O_4 crystallites (Table 2) and a lower reduction temperature (Table 3), it would be expected that it would have a higher Co metal surface area after reduction. However, the XRD analysis indicates that the GAS Co/TiO_2 Ru IMP material has a greater proportion of the Co present as cobalt titanate which cannot be reduced to Co metal under the reduction conditions used, which results in the lower Co dispersion observed.

The catalysts were screened for FT activity, and the time-online study at 210 °C is shown in Figure 6. All the catalysts showed an increase in activity over the first 5 to 10 h, as the system equilibrated. IMP Co−Ru/TiO_2 was found to have comparable activity to previous Co−Ru supported on TiO_2 catalysts tested under similar reaction conditions in the literature.[10] The GAS Co/TiO_2 catalyst then experienced a

dx.doi.org/10.1021/cs4000359 | ACS Catal. 2013, 3, 764−772

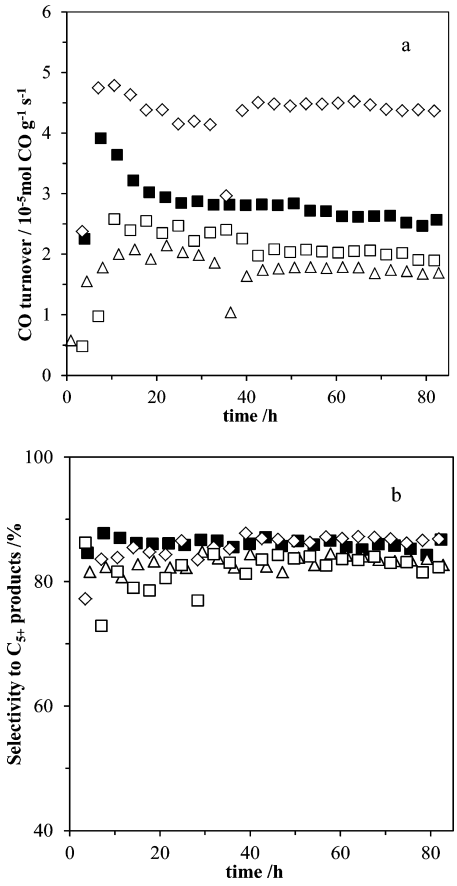

Figure 6. FT catalyst testing at 210 °C. (a) Activity; and (b) selectivity toward C_{5+} products. Reaction conditions: 210 °C, 20 bar, H_2:CO = 2:1, flows varied to give iso-conversion with values given in brackets in the key. Key: (□) IMP Co−Ru/TiO_2 (xml min^{-1}); (■) GAS Co/TiO_2 (30.1 mL min^{-1}); (◇) GAS Co−Ru/TiO_2 (30.1 mL min^{-1}); (△) GAS Co/TiO_2 Ru IMP (20.1 mL min^{-1}).

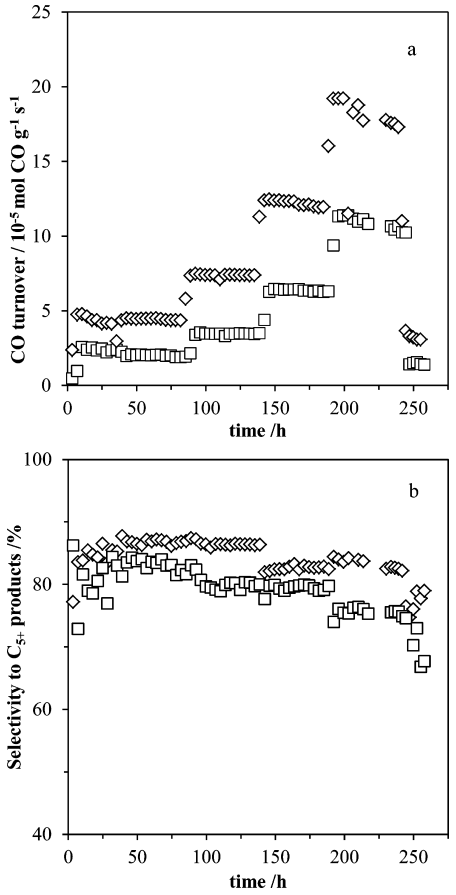

Figure 7. FT catalyst testing at 210−240 °C. (a) Activity; and (b) selectivity toward C_{5+} products. Reaction conditions: 210−240 °C, 20 bar, H_2:CO = 2:1. Key: (□) IMP Co−Ru/TiO_2; (◇) GAS Co−Ru/TiO_2.

noticeable degree of deactivation up to 20 h from 3.91×10^{-5} to 2.84×10^{-5} mol CO g_{Co}^{-1} s^{-1}, which was not observed in any of the other Ru promoted catalysts. The coking of cobalt catalysts and their partial oxidation are known deactivation mechanisms in FT reactions.[10] The prevention of the dramatic initial deactivation with the Ru promoted catalysts has previously been noted, and is ascribed to the ability of Ru to catalyze the hydrogenolysis of carbonaceous deposits and reduce surface oxygen.[10] All catalysts did display a slight drop in activity over the 80 h reaction, though this was observably less pronounced in the Co−Ru/TiO_2 GAS catalyst with activity dropping from 4.74×10^{-5} to 4.36×10^{-5} mol CO g_{Co}^{-1} s^{-1}.

All catalysts were noted to have comparable selectivity toward C_{5+} products (Figure 7b), with the GAS Co−Ru/TiO_2 clearly the most active catalyst over the 80 h reaction period, and the remaining catalysts having similar activity (Figure 7a). The GAS Co−Ru/TiO_2 had a considerably higher Co dispersion compared to the IMP Co−Ru/TiO_2 catalyst and GAS Co/TiO_2 and this correlated with the improved activity. However, the GAS Co/TiO_2 Ru IMP catalyst performed considerably poorer than expected, if the Co dispersion is taken solely as a guide to activity. An explanation, in terms of lower activity because of unreduced cobalt oxide particles, is unsatisfactory as the GAS Co/TiO_2 Ru IMP had the lowest reduction temperatures according to TPR analysis (Table 3). The difference in activity between GAS Co−Ru−TiO_2 and GAS Co/TiO_2 Ru IMP is probably due to the difference in the Co−Ru interaction, as described in the interpretation of TPR results. The enhanced mixing of Co and Ru in the GAS Co−Ru−TiO_2 catalyst leads to Co−Ru metal alloying, which has been attributed to improved FT activity.[10] It has previously been observed that catalysts with high Ru content (0.1 wt % with a 5 wt % Co catalyst) show low activity and high reducibility, relative to materials with lower Ru loading.[42] This was attributed to segregation of RuO_2 from the Co_3O_4 and adds weight to the proposal, that although discrete or surface Ru species strongly enhance reducibility, it is well mixed Co and Ru alloy that is beneficial to activity. A further study by Han et al. has also shown that phase separated RuO and Co_3O_4 facilitates reducibility, but that well mixed Ru and Co oxides provide enhanced activity through alloy formation.[43]

The GAS Co−Ru/TiO_2 catalyst that showed high activity and C_{5+} selectivity was studied over an extended temperature range of 210−240 °C, along with the IMP Co−Ru/TiO_2 catalyst (Figure 7). The Co−Ru/TiO_2 GAS catalyst was clearly the more active catalyst over the temperature range studied and remained stable up to 230 °C, before substantial deactivation occurred at 240 °C. Deactivation has frequently been observed under these conditions and is attributed to oxidation and sintering of the Co metal particles.[1] The combination of high Co dispersion and intimate mixing of Co and Ru in the GAS Co−Ru/TiO_2 catalysts has achieved in producing a catalyst that has higher activity and comparable C_{5+} selectivity to the

dx.doi.org/10.1021/cs4000359 | ACS Catal. 2013, 3, 764−772

conventionally prepared, Ru promoted, wet impregnation catalyst.

The preparation of Co/TiO_2 and $Co–Ru/TiO_2$ catalysts using GAS has been shown to be successful in terms of producing catalysts with the desired high Co loading, good Co reducibility, high Co dispersion, and excellent activity in the FT reaction. The GAS technique can utilize cobalt acetate salt as opposed to more complex and expensive Co metal salts, such as bis(cyclopentadienil)cobalt(II), that are required in supercritical deposition techniques.[36] In addition, the GAS process requires less intensive conditions of 80 bar and 25 °C compared to the 110 bar and 70 °C used in a supercritical deposition study.[36] The coaddition of Co and Ru using a supercritical fluid has not previously been reported and has been shown to produce a highly active FT catalyst.

CONCLUSION

Co/TiO_2 catalysts, with and without the addition of ruthenium as a promoter, have been prepared by GAS anti-solvent precipitation. The precipitation of metal salts formed in a slurry containing a preformed support and a solvent is reported for the first time. This GAS process allows for considerably higher metal loadings, significantly lower operating pressures and temperatures, and also less complex and cheaper metal salts than supercritical deposition techniques. The coaddition of Co and Ru to a support material using a dense gas/supercritical fluid is also reported for the first time.

The materials were tested as catalysts for the FT reaction and were found to be more active than comparable catalysts prepared by wet impregnation. This was attributed to the higher dispersion of cobalt species facilitated by the GAS precipitation methodology. The activity was particularly high for the catalyst prepared by the GAS coprecipitation of cobalt and ruthenium salts. The GAS coprecipitated Co/Ru catalyst did not have the lowest cobalt reduction temperature of the catalysts examined, a common indicator of catalyst performance, demonstrating that the ruthenium was responsible for more than just enabling hydrogen spillover to enhance cobalt reducibility. The additional affect is thought to be the formation of a Co–Ru alloy facilitated by the intimate mixing provided by the GAS technique.

ASSOCIATED CONTENT

Supporting Information

XRD patterns and quality of fit graphs are given for IMP $Co–Ru/TiO_2$, GAS Co/TiO_2, GAS Co/TiO_2 Ru IMP, and GAS $Co–Ru/TiO_2$. This material is available free of charge via the Internet at http://pubs.acs.org.

AUTHOR INFORMATION

Corresponding Author

*E-mail: Hutch@cardiff.ac.uk.

Author Contributions

Experimental work was performed by R.P.M., S.A.K., J.R.G., D.I.E., P.S., and P.B.. The work was supervised by S.A.K., T.E.D., J.K.B., G.B.C., P.B.W., S.H.T., J.B.G., and M.J.R. G.J.H. directed the research. The paper was written by S.A.K., J.K.B., and G.J.H.

Notes

The authors declare no competing financial interest.

[‖]P.B.W.: Deceased; 08/06/2012.

ACKNOWLEDGMENTS

We gratefully acknowledge funding for this work from the Technology Strategy Board. We would like to thank Johnson Matthey for their involvement in the work, with particular gratitude to Peter Williams whose support over the years has been invaluable.

REFERENCES

(1) Khodakov, A. Y.; Chu, W.; Fongarland, P. *Chem. Rev.* **2007**, *107*, 1692–1744.
(2) Schulz, H. *Appl. Catal., A* **1999**, *186*, 3–12.
(3) Reuel, R. C.; Bartholomew, C. H. *J. Catal.* **1984**, *85*, 78–88.
(4) Johnson, B. G.; Bartholomew, C. H.; Goodman, D. W. *J. Catal.* **1991**, *128*, 231–247.
(5) Ishihara, T.; Eguchi, K.; Arai, H. *J. Mol. Catal.* **1992**, *72*, 253–261.
(6) Jacobs, G.; Das, T. K.; Zhang, Y. Q.; Li, J. L.; Racoillet, G.; Davis, B. H. *Appl. Catal., A* **2002**, *233*, 263–281.
(7) Iglesia, E. *Appl. Catal., A* **1997**, *161*, 59–78.
(8) Iglesia, E.; Soled, S. L.; Fiato, R. A. *J. Catal.* **1992**, *137*, 212–224.
(9) Diehl, F.; Khodakov, A. Y. *Oil Gas Sci. Technol.* **2009**, *64*, 11–24.
(10) Iglesia, E.; Soled, S. L.; Fiato, R. A.; Via, G. H. *J. Catal.* **1993**, *143*, 345–368.
(11) Niemelä, M. K.; Krause, A. O. I.; Vaara, T.; Kiviaho, J. J.; Reinikainen, M. K. O. *Appl. Catal., A* **1996**, *147*, 325–345.
(12) Girardon, J.-S.; Lermontov, A. S.; Gengembre, L.; Chernavskii, P. A.; Griboval-Constant, A.; Khodakov, A. Y. *J. Catal.* **2005**, *230*, 339–352.
(13) Hong, J.; Marceau, E.; Khodakov, A. Y.; Griboval-Constant, A.; La, F. C.; Villain, F.; Briois, V.; Chernavskii, P. A. *Catal. Today* **2011**, *175*, 528–533.
(14) Bezemer, G. L.; Radstake, P. B.; Koot, V.; van Dillen, A. J.; Geus, J. W.; de Jong, K. P. *J. Catal.* **2006**, *237*, 291–302.
(15) Bianchi, C. L.; Martini, F.; Moggi, P. *Catal. Lett.* **2001**, *76*, 65–69.
(16) Beckman, E. J. *J. Supercrit. Fluids* **2004**, *28*, 121–191.
(17) Beckman, E. J. *Ind. Eng. Chem. Res.* **2003**, *42*, 1598–1602.
(18) Adami, R.; Osseo, L. S.; Huopalahti, R.; Reverchon, E. *J. Supercrit. Fluids* **2007**, *42*, 288–298.
(19) Haji, S.; Zhang, Y.; Kang, D.; Aindow, M.; Erkey, C. *Catal. Today* **2005**, *99*, 365–373.
(20) Lele, A. K.; Shine, A. D. *Ind. Eng. Chem. Res.* **1994**, *33*, 1476–1485.
(21) Dixon, D. J.; Luna-Barcenas, G.; Johnston, K. P. *Polymer* **1994**, *35*, 3998–4005.
(22) O'Neil, A.; Wilson, C.; Webster, J. M.; Allison, F. J.; Howard, J. A. K.; Poliakoff, M. *Angew. Chem., Int. Ed.* **2002**, *41*, 3796–3799.
(23) Reverchon, E.; Della, P. G. *Powder Technol.* **1999**, *106*, 23–29.
(24) Reverchon, E.; De, M. I.; Della, P. G. *J. Supercrit. Fluids* **2002**, *23*, 81–87.
(25) Miedziak, P. J.; Tang, Z.; Davies, T. E.; Enache, D. I.; Bartley, J. K.; Carley, A. F.; Herzing, A. A.; Kiely, C. J.; Taylor, S. H.; Hutchings, G. J. *J. Mater. Chem.* **2009**, *19*, 8619–8627.
(26) Tang, Z.-R.; Edwards, J. K.; Bartley, J. K.; Taylor, S. H.; Carley, A. F.; Herzing, A. A.; Kiely, C. J.; Hutchings, G. J. *J. Catal.* **2007**, *249*, 208–219.
(27) Hutchings, G. J.; Bartley, J. K.; Webster, J. M.; Lopez-Sanchez, J. A.; Gilbert, D. J.; Kiely, C. J.; Carley, A. F.; Howdle, S. M.; Sajip, S.; Caldarelli, S.; Rhodes, C.; Volta, J. C.; Poliakoff, M. *J. Catal.* **2001**, *197*, 232–235.
(28) Kondrat, S. A.; Davies, T. E.; Zu, Z.; Boldrin, P.; Bartley, J. K.; Carley, A. F.; Taylor, S. H.; Rosseinsky, M. J.; Hutchings, G. J. *J. Catal.* **2011**, *281*, 279–289.
(29) Tang, Z.-R.; Jones, C. D.; Aldridge, J. K. W.; Davies, T. E.; Bartley, J. K.; Carley, A. F.; Taylor, S. H.; Allix, M.; Dickinson, C.; Rosseinsky, M. J.; Claridge, J. B.; Xu, Z.; Crudace, M. J.; Hutchings, G. J. *ChemCatChem.* **2009**, *1*, 247–251.
(30) Tang, Z.-R.; Kondrat, S. A.; Dickinson, C.; Bartley, J. K.; Carley, A. F.; Taylor, S. H.; Davies, T. E.; Allix, M.; Rosseinsky, M. J.;

Claridge, J. B.; Xu, Z.; Crudace, M. J.; Hutchings, G. J. *Catal. Sci. Technol.* **2011**, *1*, 64−70.
(31) Yoda, S.; Mizuno, Y.; Furuya, T.; Takebayashi, Y.; Otake, K.; Tsuji, T.; Hiaki, T. *J. Supercrit. Fluids* **2008**, *44*, 139−147.
(32) Rietveld, H. M. *J. Appl. Crystallogr.* **1969**, *2*, 65−71.
(33) Lutterotti, L.; Chateigner, D.; Ferrari, S.; Ricote, J. *Thin Solid Films.* **2004**, *450*, 34−41.
(34) Nakamoto, K. *Infrared and Raman Spectra of Inorganic and Coordination Compounds*, 5th ed.; Wiley: New York, 1997.
(35) Lucien, F. P.; Foster, N. R. *J. Supercrit. Fluids.* **2000**, *17*, 111−134.
(36) Aspromonte, S. G.; Sastre, A.; Boix, A. V.; Cocero, M. J.; Alonso, E. *Microporous Mesoporous Mater.* **2012**, *148*, 53−61.
(37) Enger, B. C.; Fossan, A. L.; Borg, O.; Rytter, E.; Holmen, A. *J. Catal.* **2011**, *284*, 9−22.
(38) Rao, K. V.; Sunandana, C. S. *Solid State Commun.* **2008**, *148*, 32−37.
(39) Hong, J.; Chernavskii, P. A.; Khodakov, A. Y.; Chu, W. *Catal. Today.* **2009**, *140*, 135−141.
(40) Tang, C.-W.; Wang, C.-B.; Chien, S.-H. *Thermochim. Acta* **2008**, *473*, 68−73.
(41) Haller, G. L.; Resasco, D. E. *Adv. Catal.* **1989**, *36*, 173−235.
(42) Park, J.-Y.; Lee, Y.-J.; Karandikar, P. R.; Jun, K.-W.; Bae, J. W.; Ha, K.-S. *J. Mol. Catal. A: Chem.* **2011**, *344*, 153−160.
(43) Han, Q.; Yao, N.; Shi, Y.; Ma, H.; Li, X. *Catal. Commun.* **2012**, *22*, 52−57.